

**NONLINEAR LOCALIZATION AND
TURBULENCE IN MAGNETIZED
PLASMAS**

SWATI SHARMA



**CENTRE FOR ENERGY STUDIES
INDIAN INSTITUTE OF TECHNOLOGY DELHI
JULY 2016**

©Indian Institute of Technology Delhi (IITD), New Delhi, 2016

NONLINEAR LOCALIZATION AND TURBULENCE IN MAGNETIZED PLASMAS

by

SWATI SHARMA

Centre for Energy Studies

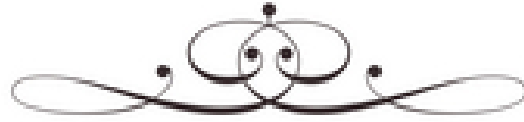
Submitted

in fulfillment of the requirements of the degree of Doctor of Philosophy
to the



INDIAN INSTITUTE OF TECHNOLOGY DELHI

JULY 2016



Dedicated to
my
Beloved Parents,
Brother
and
God



Certificate

This is to certify that the thesis entitled “**Nonlinear Localization and Turbulence in Magnetized Plasmas**” being submitted by **Ms. Swati Sharma** to the Indian Institute of Technology Delhi, for the award of the degree of *Doctor of Philosophy*, is a record of bonafide research work carried out by her. The thesis has reached the standards fulfilling the requirement of the regulations relating to the degree. The results contained in this thesis have not been submitted in part or full to any other university or institute for the award of any degree or diploma. I approve the thesis for the award of the aforesaid degree.

Date:

Dr. R. P. Sharma

Professor

Centre for Energy Studies

Indian Institute of Technology Delhi

Hauz Khas, Delhi-110016

Acknowledgments

I sincerely wish to thank and acknowledge Prof. R. P. Sharma for his generous supervision throughout my research work. His splendid guidance, fruitful suggestions, advice, constant support and encouragement provided whenever needed is much appreciated. I would also like to thank him for providing right answers to all my silly queries and giving liberty to work as suitable. It is because of his deep knowledge and physical insight of the subject this work has taken the present shape.

I am also grateful to Prof. S. Hegde, Prof. T. S. Bhatti, Dr. R. Uma and Dr. R. Narayanan, for their valuable comments and suggestions. I am also thankful to all faculty members and office staff of Centre for Energy Studies, IIT Delhi, for all type of help and cooperation during my research work. I wish to thank all my group members: Dr. Navin Kumar Dwivedi, Dr. K.V. Modi, Dr. Nidhi Gaur, Dr. Nitin Yadav, Dr. Alok Ji, Ram Kishor Singh, Nilesh Kumar Pathak, Ravinder Goyal, Hardik Pathak, Sangeeta, Anju, Neha, Saba, Prachi, Richa, Rajesh, Pradeep, Shivani for the cooperation, support and making my time there enjoyable and memorable.

I owe my deepest gratitude to my beloved father (Mr. Girish Kumar Sharma), mother (Smt. Indu Sharma), brother (Mr. Mayank Gargashya) for their unfailing love, encouragement, prayers and moral support throughout my life. Last but not least special thanks to my special friends Ashish, Kanika, Divya, Surbhi, Pratibha, Vijeyata for listening to my research issues and tolerating my annoying habits during research work at IIT Delhi.

Above all, I solicit blessings of god for progress and prosperity.

(Swati Sharma)

Abstract

The space environment consists of fully (Sun, solar wind, magnetosphere) or partially ionized plasmas (ionosphere etc) and neutral particles. The space plasma is extremely turbulent in nature and has been studied for decades using satellite observations and models. Despite these studies, the exact mechanism leading to the acceleration and heating of the solar wind is not well understood. In order to improve the understanding of physical mechanisms that are involved in these processes present study is carried out. The thesis aims towards the role played by dispersive Alfvén wave (DAW) in explaining several features observed in solar wind such as particle heating, formation of localized structures, spectral transfer of energy between different length scales etc. The dispersion in Alfvén wave is considered on account of the finite frequency correction of the wave. In finite frequency correction, we assume that the frequency of pump wave is not negligible compared with the ion cyclotron frequency. The two modes of circularly polarized DAW, left (L) and right-handed (R) fluctuations are found to behave very differently at small scales. The properties of these modes and diverse aspects of spectral transfer of wave energy over different wavenumbers is analyzed. DAW is prone to parametric instabilities such as filamentation or transverse collapse. The nonlinear interaction of DAW with other wave modes such as ion acoustic wave and magnetosonic wave is treated with ponderomotive nonlinearity using two fluid approaches. The nonlinear coupling of L and R modes; and its effect on the localized structures and resulting power spectrum is also studied in present thesis. The present research is devoted to study the nonlinear evolution of DAW in space and time using numerical techniques and semi-analytical

tools to develop basic understanding of the physics involved in DAW localization. Numerical simulation is performed to analyze the dependence of localization upon the initial wave frequency and turbulence evolution for different set of frequencies. To analyze the influence of initial condition, numerical simulation is performed by varying the initial profile of perturbation superimposed on DAW. The compressibility associated with waves such as IAW, kinetic Alfvén wave (KAW) may contribute in explaining the spectral transfer of energy at small scales. The power spectrum is studied for field and density fluctuations. The results obtained are discussed with relevance to the observations including their implication in solar wind regime.

Contents

Certificate	i
Acknowledgements	ii
Abstract	iii
List of Figures	ix
Chapter 1. Introduction	1-32
1.1. Background	1
1.2. Mathematical descriptions of Magnetized plasma	3
1.2.1. Single particle motion	4
1.2.2. MHD model	4
1.2.3. Two fluid model	8
1.2.4. Kinetic model	11
1.3. Brief outline of space and solar plasmas	12
1.3.1. Sun	13
1.3.2. Solar corona	14
1.3.3. Solar wind	15
1.3.4. Magnetosphere	17
1.4. Turbulence	19
1.4.1. Solar wind turbulence	21
1.5. Parametric instabilities of dispersive Alfvén waves	23
1.6. Spacecraft observations	24

1.7.	Objective and outline of the thesis	26
1.8.	Chapter wise summary of the thesis	29
Chapter 2.	Localization of circularly polarized dispersive Alfvén wave and Effect on solar wind turbulence	33-45
2.1.	Introduction	33
2.2.	Wave dynamics and model equations	35
2.3.	Numerical simulation and results	41
2.4.	Summary and conclusion	43
Chapter 3.	Nonlinear Coupling of Left and Right Handed Circularly Polarized Dispersive Alfvén Wave	46-66
3.1.	Introduction	46
3.2.	Model equations	49
3.3.	Semi-analytical model	53
3.4.	Numerical simulation and results	57
3.5.	Summary and conclusion	61
Chapter 4.	Temporal Evolution of Circularly Polarized Dispersive Alfvén Wave and Effect on Solar Wind Turbulence	67-85
4.1.	Introduction	67
4.2.	Dispersive Alfvén wave dynamics	69
4.3.	Magnetosonic wave dynamics	71
4.4.	Numerical simulation	73
4.5.	Semi-analytical model	77

4.6.	Summary and conclusion	81
Chapter 5. Right-handed Circularly Polarized Dispersive Alfvén Wave:		
	Localization and Turbulence in Solar Wind	86-101
5.1.	Introduction	86
5.2.	Ion acoustic wave dynamics	88
5.3.	Dispersive Alfvén wave dynamics	90
5.4.	Numerical simulation and results	93
5.5.	Summary and Conclusion	97
Chapter 6. Nonlinear Effects Related to Circularly Polarized Dispersive Alfvén		
	Wave	102-117
6.1.	Introduction	102
6.2.	Dispersive Alfvén wave dynamics	104
6.3.	Kinetic Alfvén wave dynamics	105
6.4.	Numerical simulation and results	110
6.5.	Summary and conclusion	114
Chapter 7. Nonlinear Model to Study Filamentation Instability of Dispersive		
	Alfvén Waves	118-128
7.1.	Introduction	118
7.2.	Model equations	120
7.3.	Numerical simulation and results	122
7.4.	Summary and conclusion	125

Chapter 8. Summary of the Present Work and Scope of the Future Work	129
References	134
List of research publications	142
Bio-data of the author	144

List of Figures

Figure Number	Description	Page
1.1	Plasma beta depending on the height in various regions of solar atmosphere	13
1.2	A snapshot of solar corona obtained during total solar eclipse on August 1, 2008	14
1.3	Image for the solar wind	16
1.4	Illustration of a steady state solar wind-magnetosphere system of Earth's environment in the meridian plane [Parks, 1991]	18
1.5	Schematic illustration of fluid turbulent energy spectrum	21
2.1	Transverse scale size versus critical beam power required for self trapping	44
2.2	Electric field intensity distribution of the wave (normalized by initial wave field) in x-z plane, z being the normalized distance of propagation	44
2.3	Electric field intensity profile of the wave in x-z plane obtained by numerical simulation at different pump frequencies: (a) $\omega_0 \approx 0.4\omega_{ci}$ (b) $0.6\omega_{ci}$ (c) $0.8\omega_{ci}$	45
2.4	Power spectrum of fluctuations in the electric field versus total wavenumber k for different pump frequencies: (a) $\omega_0 \approx 0.4\omega_{ci}$	45

(b) $0.6\omega_{ci}$ (c) $0.8\omega_{ci}$

- 3.1** Variation of the dimensionless beam width parameters for the pump beams (f_1 and f_2), ellipticity and Faraday rotation with z ($z = z/R_{d2}$ is the normalized distance of propagation). For the Faraday rotation case y axis is rescaled by a factor of 10^{-3} . 63
- 3.2** Electric field strength of the left (L) mode obtained semi-analytically for (a) without coupling (b) with coupling 63
- 3.3** Electric field strength of the right (R) mode obtained semi-analytically for (a) without coupling (b) with coupling 64
- 3.4** Electric field strength of the left mode in the x - z plane for a weak pump obtained numerically for (a) L mode without coupling (b) L mode with coupling 64
- 3.5** Electric field strength of the right mode in the x - z plane for a weak pump obtained numerically for (a) R mode without coupling (b) R mode with coupling 65
- 3.6** Power spectrum for the left mode pump obtained numerically for (a) HFPP left mode without coupling (b) LFPP left mode without coupling (c) LFPP left mode with coupling 65
- 3.7** Power spectrum for the LFPP right mode obtained numerically for (a) LFPP R mode without coupling (b) LFPP R mode with coupling 66
- 3.8** Power spectrum obtained numerically for HFPP modes (a) HFPP L mode with coupling (b) HFPP R mode with coupling 66

4.1	Plot of $ n_k $ versus k_x at fixed $k_z = 0$ for time (a) $t=13$, (b) $t=43$, (c) $t=50$	83
4.2	The evolution of electric field intensity of DAW with frequency $\omega_0 \approx 0.8\omega_{ci}$ in x-z plane obtained by numerical simulation for different instant of times (a) $t=13$, (b) $t=43$, (c) $t=50$	83
4.3	Saturated averaged wave number spectrum of DAW with frequency $\omega_0 \approx 0.8\omega_{ci}$ obtained between $t=28$ to $t=68$ using numerical simulation	84
4.4	The evolution of electric field intensity of DAW with pump frequency $\omega_0 \approx 0.4\omega_{ci}$ for different instant of times (a) $t=1$ (b) $t=23$ (c) $t=50$ and (d) saturated averaged wave number spectrum obtained between $t=38$ to $t=64$	84
4.5	The variation of DAW field intensity with frequency $\omega_0 \approx 0.8\omega_{ci}$ obtained semi-analytically using the amplitude of harmonics from the simulation at (a) $t=13$ (b) $t=43$ (c) $t=50$	85
5.1	The snapshots of DAW electric field intensity at fixed z at three different times (a) $t=1$ (b) $t=30$ (c) $t=38$ for two pump frequencies (i) $\omega_0 \approx 0.4\omega_{ci}$ and (ii) $\omega_0 \approx 0.8\omega_{ci}$.	98
5.2	The power spectral density of DAW plotted against wavenumber (a) k_{\perp} at time $t=43$ and $t=30$ and (b) k_{\parallel} at time $t=47$ and $t=33$ as turbulence is attained, for pump frequencies $\omega_0 \approx 0.4\omega_{ci}$ and	99

$\omega_0 \approx 0.8\omega_{ci}$ respectively

- 5.3** The snapshots of DAW electric field intensity at fixed z at three different times (a) $t=1$ (b) $t=20$ (c) $t=28$ for two pump frequencies (i) $\omega_0 \approx 0.4\omega_{ci}$ and (ii) $\omega_0 \approx 0.8\omega_{ci}$ with different initial wave profile. 100
- 5.4** The power spectral density of DAW plotted against wavenumber (a) k_{\perp} at time $t=28$ and $t=20$ and (b) k_{\parallel} at time $t=30$ and $t=23$ as turbulence is attained, for pump frequencies $\omega_0 \approx 0.4\omega_{ci}$ and $\omega_0 \approx 0.8\omega_{ci}$ respectively, with different initial wave profile. 101
- 6.1** The electric field intensity of DAW in x - y plane at fixed z for (a) $\alpha_x, \alpha_y, \alpha_z = 0.1$ (b) $\alpha_x, \alpha_y, \alpha_z = 0.2$ and (c) $\alpha_x, \alpha_y, \alpha_z = 0.4$ at (i) initial time ($t=1$) and (b) $t=35$. Here, $|A_0|=1$ and $\varepsilon=0.1$ for all the three cases. 115
- 6.2** The evolution of DAW intensity for a low pump wave amplitude, $|A_0|=0.6$ and wavenumber of perturbation, $\alpha_x, \alpha_y, \alpha_z = 0.2$ at three snapshots of time (i) $t=1$, (ii) $t=32$ and (iii) $t=38$ respectively. 115
- 6.3** (a) The plot of DAW intensity in x - y plane for pump frequency $\omega_0 \approx 0.5\omega_{ci}$ shown by means of snapshots at different times (i) $t=1$ and (ii) $t=25$ and (iii) $t=27$, with (b) respective contour plots. 116
- 6.4** (a) The evolution of DAW intensity with time in x - y plane for pump 116

frequency $\omega_0 \approx 0.8\omega_{ci}$ shown by means of snapshots at different times (i) $t=1$ and (ii) $t=20$ and (iii) $t=23$, with (b) respective contour plots.

- 6.5** Spectra of density fluctuations versus wave number. The power spectral scaling is shown for reference. 117
- 6.6** The saturated average wave number spectrum of DAW obtained by plotting $\langle |A_k|^2 \rangle$ against k . These spectra were obtained using 20 spectra i.e., (a) between $t=22$ and 42 for pump frequency $\omega_0 \approx 0.5\omega_{ci}$ and (b) between $t=18$ and 38 for pump frequency $\omega_0 \approx 0.8\omega_{ci}$ respectively. 117
- 7.1** Evolution of energy content of three Fourier modes, $|\tilde{E}_{1k}|$ at $k_x = 0, k_x = \alpha$ and $k_x = 2\alpha$ respectively and fixed k_y , with z for (a) typical NLS case showing FPU recurrence and (b) present system. 126
- 7.2** The variation of electric field intensity of perturbation in (1) x-z plane (for fixed y) and (2) y-z plane (for fixed x) for different values of α_x, α_y i.e., (a) $\alpha_x, \alpha_y = 0.1$, (b) $\alpha_x, \alpha_y = 0.2$ and (c) $\alpha_x, \alpha_y = 0.6$ for $\gamma=2$ 126
- 7.3** The snapshots of (a) electric field intensity evolution of the 127

perturbation at three values of z , (i) $z=1$, (ii) $z=15$ and (iii) $z=48$ respectively, for case $\gamma=2$ and $\alpha_x, \alpha_y=0.2$, and (b) respective contour plot

- 7.4** The variation of electric field intensity of perturbation for (i) $\gamma=1$ and 127
(ii) $\gamma=3$ in (a) x-z plane (for fixed y) and (b) y-z plane (for fixed x)
respectively for $\alpha_x, \alpha_y=0.2$
- 7.5** The variation of $|\tilde{E}_{1k}|^2$ along wave number k for different pump 128
amplitude (a) $\gamma=1$ (at $z=80$) and (b) $\gamma=3$ (at $z=108$).